CLM-P62

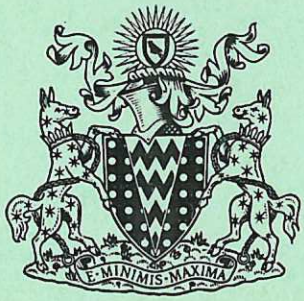

United Kingdom Atomic Energy Authority

RESEARCH GROUP

Preprint

A MICROWAVE INTERFEROMETER FOR THE MEASUREMENT OF SMALL PHASE ANGLES

E. HOTSTON
M. SEIDL

Culham Laboratory,

Culham, Abingdon, Berkshire

1964

UNCLASSIFIED
(Approved for publication)

CLM - P62

A MICROWAVE INTERFEROMETER FOR THE MEASUREMENT OF SMALL PHASE ANGLES

by

E. HOTSTON
M. SEIDL*

(Submitted for publication in J. of Scientific Instruments)

ABSTRACT

A microwave interferometer has been developed to measure the small phase changes produced in a microwave traversing a fully ionized gas. The interferometer can detect phase changes of 1.2° with a repeatability of 0.1°. It has been calibrated for phase angles in the range 5° to 40°, to an accuracy of 6% over the frequency range 8080 - 11510 Mc/s. The interferometer is insensitive to absorption of energy from the microwave beam by the ionized gas, and uses a balanced output to reject electrical interference.

The interferometer has been used to estimate the electron density of a tenuous plasma ($4.10^{10} cm^{-3}$) over a 10 cm path length, with a time resolution of 10^{-6} sec.

*On leave from the Institute of Vacuum Electronics,
Czechoslovak Academy of Sciences, Prague.

U.K.A.E.A. Research Group,
Culham Laboratory,
Nr. Abingdon,
Berks.

September, 1964. (C/18 JG)

CONTENTS

		Page
1.	Introduction	1
2.	The Interferometer	1
3.	The Adjustment of the Interferometer	2
4.	The Theory of the Interferometer	3
5.	Calibration Experiments	7
6.	Interpretation of the Results	9
7.	The Measurement of Time Dependent Phase Angles	11
8.	Experiments with MTSE	14
9.	Conclusions	17
	Acknowledgements	17
	References	18

TABLES

Table I	Measured Values of Phase Shift and Refractive Index for Blocks of Polystyrene Foam of Thickness ℓ	19
Table II	Values of Phase Shift and Dielectric Constant for Single Sheets of Polystyrene and Polythene when inserted between the Interferometer Horns.	19
Table III	Value of Sin θ measured for Rectangular Blocks of Polystyrene Foam of thickness 10 cm and sides a, b with side b parallel to the Electric Vector, (Sin θ from equation 10)	20
Table IV	Variation of the Correction Factor C with the Open Circuit Output Voltage of a Crystal Detector for a value of θ of 30°	20
Table V	Value of Phase Shift and Peak Electron Density found for the M.T.S.E. Plasma	21

Errata

Abstract	line 2, after 'microwave' insert 'beam'
p1.	line 6, for 'state' read 'static'
p6.	in last equation, for 'Sin $(\eta - \xi)$' read 'Sin $(\eta + \xi)$'
p12.	line 12, for 'θ' read 'θ_1'
p12.	line 13, for 'Sin θ = C Sin θ' read 'Sin θ_1 = C Sin θ'
p16.	line 1, after 'shift' insert 'varied'
p17.	line 26, for 'Jenkins' insert 'Jenkin'

1. Introduction

A common method of estimating plasma electron density is to measure the refractive index μ for transverse electromagnetic radiation, which is related to the density by (Radcliffe 1959)

$$\mu^2 = 1 - 8 \cdot 1 \cdot 10^7 \, n \, f^{-2}, \qquad \ldots (1)$$

where n is the electron density (cm^{-3}) and f the frequency (sec^{-1}), and the effects of a quasi-state magnetic field in the plasma are neglected. Equation (1) also assumes that there is no absorption of energy from the radiation by the plasma. For laboratory work using microwaves it has been usual either to work with μ close to zero and to observe the time at which transmission begins, or to measure μ by an interferometer using path lengths and wavelengths chosen to give many fringe shifts. (Harding et al. 1958, Wharton 1961).

The present paper describes a novel interferometer which has been developed to measure small phase shifts, so that low plasma densities could be measured over short path lengths using wavelengths short compared with the plasma dimensions, a requirement which arose in the Magnetic Trap Stability Experiment (MTSE) (Francis, Hill, Mason, 1964) at Culham. To judge from a recent review (Harvey 1963) this interferometer has a number of useful features: it can measure phase changes in the range 1° - 40° with an accuracy of 10%; it has a resolving time of less than 1 microsecond; and it is insensitive to absorption of microwave energy by the plasma and to interference from violent sources. It has been operated in the 3 cm band to measure electron densities up to $5 \cdot 10^{10} cm^{-3}$ over a 10 cm path length.

2. The Interferometer

Fig.1 shows the interferometer in the form in which it was used on a microwave test bench, when the calibration experiments described

below were carried out. With the exception of the waveguide horns it was constructed from standard X-band waveguide components. Power from the klystron oscillator 0, (EMI type 25182) connected to a voltage stablised power supply (Solartron type AS 962), entered the shunt arm of the hybrid tee E and was split into two equal beams; the series arm of the tee was terminated by a matched load. One of the beams leaving the tee E formed a reference beam and was sent by the path E A B F to the shunt arm of a second hybrid tee F; this path contained a 90° twist section to rotate the plane of polarisation of the wave. The other wave leaving E was used to probe the material whose refractive index was required; it passed by the path E C H_1 H_2 F and entered the hybrid tee F by the series arm; H_1, H_2 were waveguide horns of 7.3 × 3.5 cm^2 aperture and 8.7 cm length; the electric vector of the wave was parallel to the 3.5 cm side of the horn. The waveguide run E A B F contained two attenuators G_1, G_2, and a phase shifter J. Ferrite isolators K were inserted into the waveguides as shown. The two remaining arms of the hybrid tee F were connected to short lengths of waveguide FP, FQ, terminated by crystal detectors M_1 and M_2 of square law response whose output currents were displayed on galvanometers of 450 ohm resistance.

3. The Adjustment of the Interferometer

The interferometer was adjusted, by cutting off the reference beam by the attenuators G_1, G_2, so that the power of the reference beam entering the tee F was undetectable. The crystal currents x_1, y_1 in M_1 and M_2 caused by power propagating between H_1 and H_2 were measured. Next the probe beam was cut off by placing a metal screen between H_1 and H_2; the isolator behind the horn H_1 and the hybrid tee E ensured that any power reflected from the screen into the horn did not penetrate into the waveguide E A B F; similarly the level setting attenuator N and its associated isolator

prevented any reflection of power back into the oscillator O. The isolator situated between H_2 and F prevented any power reflected from the waveguides FP, FQ back into the waveguide H_2F from being reflected from the screen back into F. With the metal screen in place the attenuation in the arm E A B F was adjusted and the reference beam restored until the crystal currents x_2, y_2 were as nearly as possible equal respectively to x_1 and y_1. Finally, transmission between the horns was restored and the phase shifter J adjusted so that crystal currents X_O, Y_O due to both probe and reference beams as nearly as possible obeyed the relationship

$$X_O = x_1 + x_2 \qquad Y_O = y_1 + y_2 \qquad \ldots (2)$$

Failure to obey the conditions $x_1 = x_2$, $y_1 = y_2$ and equation 2 exactly may be explained if the hybrid tee F were of asymmetrical construction, or if there were coupling between the detector arms FP, FQ such that some of the power flowing from F to P were reflected back towards F and a portion of this eventually reached Q. The theory given below allows these effects to be dealt with rigorously, and it shows that if a transparent obstacle were placed between H_1 and H_2 so as to change the phase of the wave entering the horn H_2 by an angle θ, then the crystal currents change from X_O, Y_O to X, Y where to a first approximation

$$\text{Sin } \theta = \pm \frac{\frac{X}{X_O} - \frac{Y}{Y_O}}{\frac{X}{X_O} + \frac{Y}{Y_O}} \qquad \ldots (3)$$

4. The Theory of the Interferometer

The operation of the interferometer may be understood by reference to the appropriate index diagrams, Fig.2. The notation is such that the wave in the waveguide FP flowing from F to P gives rise to the crystal currents denoted by x, and the wave from F to Q to the currents y.

Consider first the case of a symmetrical tee F and no coupling between FP and FQ. The amplitude of the wave from F to P when the reference beam was cut off is represented by the line pp_1, Fig.2a, and the amplitude of the wave when the probe beam was cut off by the line pp_2, when both beams propagate along FP the resultant wave is represented by the diagonal pp_3 of the parallelgram defined by pp_1, pp_2, the phase between the components pp_1, pp_2 which is varied by the phase shifter J is the angle $\frac{1}{2}\pi + \alpha$. The corresponding waves in the guide FQ are represented by qq_1, qq_2, qq_3, Fig.2b; the phase angle between qq_1 and qq_2 is now $\frac{1}{2}\pi - \alpha$, because of the properties of the hybrid tee. Since the detectors at P, Q are of square law response the crystal currents are proportional to the squares of the lengths of the lines in the index diagrams, so that

$$X_O = x_1 + x_2 - 2\sqrt{x_1 x_2}\ \text{Sin}\ \alpha$$
$$Y_O = y_1 + y_2 + 2\sqrt{y_1 y_2}\ \text{Sin}\ \alpha \qquad \ldots (4)$$

Equations 2, ($X_O = x_1 + x_2$, $Y_O = y_1 + y_2$) will be satisfied if the phase shifter J is adjusted so that $\alpha = m\pi$ where m is zero or an integer. Now suppose that a transparent obstacle is placed between H_1 and H_2 which changes the phase of the wave entering H_2 by θ and its power by a factor $(1-\Delta)^2$ where Δ is a dimensionless factor. The introduction of the obstacle results in a change in the index diagrams. The lines pp_1, qq_1 which represent the amplitudes of the component waves in FP, FQ due to the probe beam, are both rotated through an angle θ, and are shortened in length by a factor $(1-\Delta)$, so that they now become pp_4, qq_4. The crystal currents X, Y are proportional to the squares of the resultant amplitude pp_5, qq_5 so that

$$X = x_1 (1-\Delta)^2 + x_2 - 2\sqrt{x_1 x_2}\ (1-\Delta)\ \text{Sin}\ (\alpha+\theta)$$
$$Y = y_1 (1-\Delta)^2 + y_2 + 2\sqrt{y_1 y_2}\ (1-\Delta)\ \text{Sin}\ (\alpha+\theta) \qquad \ldots (5)$$

If the interferometer was adjusted so that $x_1 = x_2$, $y_1 = y_2$ and $\alpha = m\pi$ equations 4 and 5 may be combined to produce

$$\text{Sin}\,\theta = (-1)^{m+1}\left[1 + \tfrac{1}{2}\Delta^2\,(1-\Delta)^{-1}\right]\frac{\frac{X}{X_o} - \frac{Y}{Y_o}}{\frac{X}{X_o} + \frac{Y}{Y_o}} \qquad \ldots (6)$$

Equation 6 reduces to equation 3 if $\Delta = 0$ and there is no attenuation of the wave by the obstacle. Equation 6 shows that the interferometer is not sensitive to the attenuation of the wave by the obstacle.

Next consider the case where there is no attenuation of the wave by the obstacle so that $\Delta = 0$, but where the hybrid tee or the detection system is imperfect, that is the hybrid tee is asymmetrical or there is coupling between the arms FP, FQ, so that waves reflected back towards F along one arm give rise to a wave in the other arm. The index diagram for the arm FP is Fig.2c; and for arm FQ, Fig.2d. The notation is the same as the previous case, pp_1, pp_2 representing the waves flowing from F towards P when the reference and probe beams were cut off respectively, and $\frac{1}{2}\pi + \alpha$ the phase angle between the component waves when both beams are propagating. As before α can be varied by adjustment of the phase shifter J but will also vary if the coupling between the arms FP, FQ is altered, in what follows the coupling will be assumed constant. The index diagram 2d, for the arm FQ is similar to the diagram 2b, except that the angle between qq_1 and qq_2 is no longer $\frac{1}{2}\pi - \alpha$ but $\frac{1}{2}\pi - (\alpha+\gamma)$ where γ is an angle, much less than $\frac{1}{2}\pi$; which represents the effect of the imperfections of the system. The resultant waves in the arms FP, FQ are determined as before, and the crystal currents X_o, Y_o are

$$X_o = x_1 + x_2 - 2\sqrt{x_1 x_2}\ \text{Sin}\,\alpha$$

$$Y_o = y_1 + y_2 + 2\sqrt{y_1 y_2}\ \text{Sin}\,(\alpha+\gamma) \qquad \ldots (7)$$

Changing the phase of the wave entering H_2 by means of a transparent obstacle between H_1 and H_2, results in a rotation of the lines pp_1, qq_1 by an angle θ, so that they become pp_4, qq_4, the crystal currents X, Y are now

$$\begin{aligned} X &= x_1 + x_2 - 2\sqrt{x_1 x_2}\ \text{Sin}\ (\alpha+\theta) \\ Y &= y_1 + y_2 - 2\sqrt{y_1 y_2}\ \text{Sin}\ (\alpha+\gamma+\theta) \end{aligned} \qquad \ldots (8)$$

The initial adjustment of the interferometer with the phase shifter J results in α becoming approximately equal to $m\pi$, when m is zero or an integer, it is convenient to replace α, γ, by angles η, ξ, which lie in the range $\frac{1}{4}\pi$, $-\frac{1}{4}\pi$, where

$$\begin{aligned} \alpha &= m\pi - \eta + \xi \\ \alpha + \gamma &= m\pi - \eta - \xi \end{aligned} \qquad \ldots (9)$$

Equations 7, 8, 9 after some manipulation result in the following relations between θ the phase change, and the observed crystal currents

$$\text{Sin}\ \theta = (-1)^{m+1}\ \frac{S - (1-\text{Cos}\theta)\left[\dfrac{x_1 + x_2 - X_o}{2X_o}(1-S) - \dfrac{y_1 + y_2 - Y_o}{2Y_o}(1+S)\right]}{(1-S)\dfrac{\sqrt{x_1 x_2}}{X_o}\text{Cos}\ (\eta-\xi) + (1+S)\dfrac{\sqrt{y_1 y_2}}{Y_o}\text{Cos}\ (\eta+\xi)} \qquad \ldots (10)$$

where

$$S = \frac{\dfrac{X}{X_o} - \dfrac{Y}{Y_o}}{\dfrac{X}{X_o} + \dfrac{Y}{Y_o}} \qquad \ldots (11)$$

and

$$\begin{aligned} \text{Sin}\ (\eta - \xi) &= (-1)^m\ \frac{X_o - (x_1 + x_2)}{2\sqrt{x_1\ x_2}} \\ \text{Sin}\ (\eta - \xi) &= (-1)^{m+1}\ \frac{Y_o - (y_1 + y_2)}{2\sqrt{y_1\ y_2}} \end{aligned} \qquad \ldots (12)$$

5. Calibration Experiments

The interferometer of Fig.1 was calibrated by placing sheets of low loss dielectric material between the horns of the interferometer and comparing where possible, the measured values of phase shift with those calculated from published values of dielectric constant. Where published values of dielectric constants were not available values of phase shift which were self-consistent to within ± 6% over a frequency range of 3400 Mc/s at a mean frequency of 9700 Mc/s were taken to indicate that the interferometer was operating in a satisfactory manner. This procedure did not differentiate between the various sources of error in the interferometer but measured the overall performance. The crystal currents were kept to 1.0 microamp or less. After the interferometer had been adjusted, the galvanometers were observed to show small, erratic variations in their deflections, whose time constant was of many seconds duration. It was estimated that at their worst these variations would limit the accuracy of any one measurement of phase to 0.7°. This was an acceptable figure, as estimates of the phase shift to be expected with the Magnetic Trap Stability Experiment, based on its design parameters lay in the range 5° to 50°. The variations are due to fluctuations in the output of the klystron oscillator due to small variations in the output voltages of the stabilised power supply operating it. The limit of accuracy of 0.7° arises because the time required to make a calibration 30 to 60 sec. was comparable to the time scale of the fluctuations. As discussed below, if the phase shift is measured in a time short compared with the time scale of the fluctuations, the repeatability of the measurements of phase is better than ± 0.1°.

The first calibration experiment was to place a block of polystyrene foam 30 cm square, 10 cm thick midway between the horns of the interferometer and make five separate determinations of phase

shift at a frequency of 9310 Mc/s, the measured values of phase shift (equation 3) lay in the range 9.45° to 10.13°, with a mean value of 9.7° and a mean deviation of 0.2°. Next the polystyrene foam block was moved along the axis of the horns starting with its face 5.2 cm away from the transmitting horn and finishing 8.7 cm away. The phase shift was measured at eight equi-spaced positions in this interval. The mean value of phase shift was 10.1° and all the observations lay in the range 9.6° to 10.2°. Further, the phase shift was measured with the polystyrene block on contact with both transmitting and receiving horns, again the mean value of phase shift was 10.1°. In the above measurements the approximate expression for phase shift (equation 3) was used, as the correction is small (see table I) and relative values only were required. These measurements showed that the position of the polystyrene foam block between the interferometer horns was not critical and, hence, that the radiation field between the horns could be regarded as a plane progressive wave if the obstacle causing the phase shift were several wavelengths thick and had a refractive index of near unity.

The phase shift as measured by the interferometer was now investigated as a function of phase shift introduced by placing obstacles between the horns. Sheets of polystyrene foam 30 cm square 5, 10, 20 cm thick were introduced between the horns and the phase shift measured: the results are presented in table I.

The dielectric constant of polystyrene foam is not known with sufficient accuracy so an attempt was made to obtain an absolute calibration by inserting sheets of a known dielectric constant between the horns. Using materials such as these, whose dielectric constant differs appreciably from unity, introduces a complication. The receiving horn H_2 did not pass all the microwave energy falling on to it to the hybrid tee F, but reflected some of it back to H_1

which in its turn reflected a small portion of this reflected radiation back to H_2, giving rise to a standing wave between the horns. This standing wave had a small amplitude compared with the progressive wave. Insertion of a sheet of dielectric material between the horns interfered with this standing wave. The energy reflected from H_2 suffered partial reflection from the dielectric sheet and was returned to H_2 and was transmitted to the tee F, the phase of the resultant wave which entered F was then a function of the separation of the dielectric sheet from H_2. A full analysis of the situation required that the phase of a wave propagating through a region containing four partially reflecting surfaces be computed. It is clear that the result of such a computation would show that the phase of the wave entering F by way of H_2 would show a periodic variation as the separation of the dielectric sheet from H_2 or H_1 is increased. This variation was observed, and measurements of phase shift were made, for various values of z (the separation of the dielectric sheet from H_1) at intervals of 0.8 cm or 0.5 cm. The results of these observations are given in Table II, which lists both the mean values of phase shift and the mean deviation.

Finally the radiation pattern from the horns was investigated by suspending blocks of polystyrene foam 10 cm thick between the horns and measuring the phase shift produced. The blocks were of rectangular cross section (a,b) with the side b parallel to the electric vector of the wave. The values of sin θ for the various blocks are given in Table II, it would appear that measurements of phase shift produced by a plasma column 10 cm diameter should not be in error by greater than 15% because of geometrical factors.

6. Interpretation of the Results

The phase shift observed in the calibration experiments have been used to calculate the refractive index μ, of the sheets of

polystyrene, polythene and polystyrene foam. The refractive indices found for the polystyrene foam are given in Table I; Table II lists values of the dielectric constant μ^2 for the sheets of polystyrene and polythene.

The phase shift θ caused by placing a parallel sided sheet of dielectric of thickness ℓ between the horns of the interferometer has been shown to be (Redheffer 1947).

$$\theta = \phi - \beta_o \ell$$

where

$$\tan \phi = \tfrac{1}{2} \left[\mu + \mu^{-1} \right] \tan \mu\beta_o \ell$$

and $\beta_o = 2 \pi \lambda^{-1}$, where λ is the wavelength of the radiation of air. The results quoted assume that none of the microwave power falling on the horns H_1, H_2 is reflected or scattered. A simplification is possible if the refractive index is near unity, which is the case for the polystyrene foam, in this case $\theta = (\mu - 1) \beta_o \ell$.

The dielectric constants of polystyrene and polythene vary by less than 0.5% over the frequency range 3000-10,000 Mc/s (Von Hippel 1954) although there is a variation of dielectric constant between specimens of different manufacture. The dielectric constant of polythene lies in the range 2.24 - 2.31 (Von Hippel 1954) and that for polystyrene in the range 2.53 - 2.56 (Von Hippel 1954, Hotston 1961).

From Table I, the mean value of $(\mu - 1)$ for polystyrene foam is $9.1\ 10^{-3}$ and is constant to $\pm$ 6% over the frequency range 8080-11510 Mc/s. This is interpreted as showing that the interferometer can measure phase angles of from 5° to 20° to an accuracy of $\pm$ 6% over the above frequency range. These tests most nearly simulate the effects of the plasma, as the refractive index is nearly unity. The measured values of dielectrics constant in Table II are consistently

higher than those quoted above by approximately 5%. For the polythene sheet at a frequency of 9370 Mc/s an error of 1.5° in the measurement of phase results in an error of 0.10 in the dielectric constant; for the polystyrene sheet a 1.5° error in phase results in an error of 0.11 in the dielectric constant. The cause of the discrepancy between measured and published values is thought to be the assumption that the effect of reflection of radiation from the horns may be neglected if the average value of phase shift is taken. Table II does however show that the accuracy of refractive index determination is better than 5% at 40°.

7. The Measurement of Time Dependent Phase Angles

To measure time dependent phase angles the crystal detector signals were displayed on an oscilloscope. If the crystals are matched for sensitivity, balanced amplifiers may be used in a double beam oscilloscope, one beam being used to display the sum of the crystal signals, and the other the difference signal. Since in many cases the sum signal is approximately constant, the difference signal gives, to a sufficient degree of accuracy for many purposes, a direct display of phase angle.

Since the output of the crystals is balanced with respect to each, and any electrical interference which is encountered will be the same sign for both crystals, the balanced amplifier will reject this interference superimposed upon the difference signal. When measuring small phase angles caused by low density plasmas, the interference level on the sum signal is not as important as that on the difference signal, since the sum signal is by far the larger of the two signals. The balanced output of the interferometer with its ability to reject unwanted interference, enables it to work in conditions where the interference level is too high for a single detector interferometer to operate.

It was sometimes necessary to operate the crystal detectors in a region where they depart from their square law characteristic and subsequently make a correction for this effect. Because the crystals operate into a high impedance amplifier the correction is expressed in terms of the open circuit output voltage of the crystals. The correction factor can be calculated if the graphs of output voltage against input power for the crystals are plotted. Little experience has been gained of the variation of crystal characteristics from crystal to crystal, but it has been possible to choose crystals whose characteristics agreed to within 1% in the region where the output voltage varied from 0.13v to 0.38v. With matched crystals it is found that the phase shift θ, calculated from equation 10 is lower than the true value θ, the relation can be written $\text{Sin } \theta, = C \text{ Sin } \theta$, where C is a correction factor. For an open circuit output voltage of 0.25v, C remains constant to better than 4% for values of θ varying from 5° to 30°. C is however a function of output voltage; table IV gives what would appear to be a typical variation of C for a value of θ of 30°.

Some tests of the oscilloscope display were performed on an interferometer which resembled that of Fig.1; except that its dimensions were larger, and that the path of the microwaves through the air between the horns H_1 H_2 of Fig.1 was replaced by a length of oversize waveguide. The oversize waveguide was 32.5 cm long and 9.9 x 15 cm^2 internal dimensions, the transitions to the standard 3 cm guide was by means of tapers 30 cm long. The oversize waveguide was in two sections each 15 cm long with a gap 2.5 cm wide between them, through this gap a sheet of polystyrene foam could be passed on the end of a pendulum, to produce a small transient phase shift in the probe beam, the time case of the cathode ray oscilloscope was triggered at the start of the oscillations of the pendulum.

The crystals which were a matched pair were connected to the oscilloscope by a resistance capacity network of 6 sec time constant. The difference amplifier of the oscilloscope was directly coupled, the manufacturers stated that its high frequency limit had a nominal value of 300 Kc/s [3 db. point].

After adjusting the oscilloscope, experiments were performed at a frequency of 9400 Mc/s. The polystyrene foam sheet was allowed to pass through the gap in the waveguide and the difference of the crystal signals displayed on the oscilloscope and recorded. Fig.3 shows a typical result, the polystyrene sheet made three traverses through the gap between the oversize waveguides in a time of 1 sec. [the duration of the time base]; to show the reproducability of the system three traces have been overlaid. The sum of the crystal signals was not recorded as it was known to remain constant to within the limit of observation, ± 5%. The phase shift produced by the polystyrene sheet at its second transit through the gap in the waveguides is found from Fig.3 to be 1.2°, the repeatability of the measurement being better than 0.1°. The repeatability of the initial adjustment was also about 0.1°. Table I shows that at a frequency of 9410 Mc/s a phase shift of 1.3° would be expected from a sheet of polystyrene foam 1.2 cm thick, which is satisfactory agreement.

When performing measurements with a plasma containing device there will be a time lag of up to several minutes between adjusting the interferometer and measuring the phase shift produced by the plasma. During this time the interferometer may drift out of adjustment due to variations in the output of the klystron, this source of error has been eliminated as follows. Variations in the klystron output will affect both its power and its frequency. The variations in power are of no importance if the power level is monitored continuously, this was done by displaying the sum of the crystal signals

on an oscilloscope with a directly coupled amplifier. Variations in frequency will, if the optical path of the probe and reference beams are unequal, result in variations of the difference signal. It was found that varying the reflector voltage about its optimum value changed the frequency of the klystron by an amount sufficient to cause the difference signal of the interferometer to change by an amount corresponding to a phase shift greater than 9°. This phase shift was more than ten times the drift of the interferometer from all causes. Measurements of the phase shift produced by the polystyrene foam sheet attached to the end of the pendulum, for various values of the reflector voltage, showed that the frequency change produced by a 10v variation of the reflector voltage resulted in a 10% change in the measured value of the phase shift. From this it was concluded that any errors due to frequency drift of the klystron would be negligible.

8. Experiments with MTSE

The Magnetic Trap Stability Apparatus consists of a glass drift tube 22.9 cm internal diameter along which a plasma blob is guided by an axial magnetic field. At a point 3 metres distant from the gun the plasma enters a magnetic trap formed by the electric currents in two circular coils coaxial with the drift tube, in this instance the coils were 1 metre apart. The current in the coil nearest the gun was pulsed on when the plasma passed through the coil, the other coil was permanently energised. The current carrying bars external to the drift tube which created the hexapole stablising field were in this case not fitted. The interferometer horns identical with those of Fig.1 were placed 24 cm apart at the ends of a diameter of the drift tube, the electric vector of the probe beam was parallel to the static magnetic field, so that the relation between refractive index and plasma density was given by equation 1. The interferometer used

is shown in Fig.4 and differed from that of Fig.1, in that the hybrid tee E used as a beam splitter was replaced by a directional coupler, and that the ferrite isolators were fitted in front of the crystal detectors. The crystal detectors were connected to directly coupled emitter follower amplifiers whose output was fed to a double beam oscilloscope in a screened room. The oscilloscope had directly coupled amplifiers and displayed the sum and difference of the crystal signals. The rise time of the oscilloscope amplifiers was 0.01 microsecond, the frequency response of the emitter followers was not measured as the designed upper frequency limit was in excess of 10 Mc/s [3 db. point], so that resolving times of less than 1 microsecond were obtained. The oscilloscope was triggered from a pulse derived from the current operating the plasma gun a suitable delay being incorporated. The crystal detectors and emitter followers were screened by placing them in a copper box, connection to the screened room being by coaxial cables contained in copper tubes.

The interferometer was tested before it was attached to the MTSE apparatus by using it to measure the phase shift produced by a polystyrene sheet 0.157 cm thick, the measured value was 11°, the value calculated using the value of dielectric constant given in Table II is 11.4°, the values of dielectric constant of 2.24 to 2.31 given by Von Hippel correspond to phase shifts of 10.4° to 10.8°.

Fig.5 is a typical oscillogram obtained with the MTSE apparatus. Placing a polythene sheet between the waveguide horns and the drift tube caused the difference signal to change in the opposite sense to that of the figure, showing the refractive index of the plasma to be less than unity. The peak phase shift was calculated from the oscillograms, and the refractive index and plasma density calculated assuming a uniform plasma 10 cm thick. Because the plasma gun

operated irreproducably the measured values of phase shift from shot to shot, by up to a factor of three. The results are summarised in Table V which also gives the mean and standard deviations of the phase angle, and the mean electron density. The slight diminution of the sum signal which occurs in the first 30 microseconds of the trace is absent in oscillograms which show a smaller phase shift; it is interpreted as a change in the signal level of the probe beam as it crossed the plasma. The small oscillation at a frequency of approximately 1 Mc/s occurring in the sum signal and the spike 17 microseconds after the beginning of the trade are electrical interference from the aforementioned gate coil, and provide a reference for timing. In the first 17 microseconds of the trace a steady increase in phase shift is observed as the plasma enters the magnetic trap, after the trap is closed at 17 microseconds there is an increase in density, followed by a decay as the plasma escapes from the magnetic trap (Francis et al 1964).

Other assumptions regarding the shape and size of the plasma give different values of the density of the plasma, for a given phase shift. A more realistic assumption than that of a uniform plasma 10 cm thick, is that of a plasma column 10 cm diameter with a parabolic density distribution such that the density a distance r cm from the axis is $n = n_o (1-0.04r^2)$ where n_o is the central density. The phase shift produced by this distribution has been calculated (Wort 1963): if n_1 is the density calculated from the observed phase shift assuming a uniform plasma, then the corresponding densities of the parabolic distribution are, peak density $n_o = 1.5\, n_1$, and mean density $= 0.75\, n_1$. The analysis used assumes that the plasma dimensions are large compared with the wavelength; this is not the case with the present interferometer used with the MTSE plasma. If the plasma is assumed to have an equivalent thickness of 7.5 cm,

Table III indicates that the systematic error due to neglect of diffraction effects will be of the order 10%. If the measured values of phase shift are assumed to have a normal distribution about their mean value, then 68% confidence limit is ± 8% of the mean value.

9. Conclusions

A new type of microwave interferometer has been developed to measure small phase shifts. Laboratory tests have shown that phase angles of 1.2° can be measured with a repeatability better than ± 0.1°. The interferometer has been calibrated for a range of phase shifts from 5° to 40° and has been shown to have an accuracy of better than ± 8%. The interferometer is insensitive to changes in the attenuation of the probe beam by the object whose refractive index is being measured. The chief sources of error are multiple reflections and diffraction effects.

The interferometer has been used to estimate the electron density of the plasma in the Magnetic Trap Stability Experiment, assuming a parabolic density distribution in a plasma column 10 cm diameter, the mean plasma density was found to be $3.7 \times 10^{10} cm^{-3}$, with a possible systematic error of ± 10% due to neglect of diffraction effects, and a further error of ± 8% (68% confidence limit) due to statistical fluctuations in the output of the plasma gun.

Acknowledgements

The authors would like to thank the following members of the Culham Laboratory Staff: Dr G. Francis for facilities on the MTSE assembly and members of his group, especially Mr C.D. King and Mr R. Jenkins of the electronics Division.

We would also like to thank Dr R.S. Pease, Mr D. Wort, Mr J. Weaver and Mr J. Schofield for much helpful advice and constructive criticism.

References

Francis, G., et al., 1948, Nature, 203, 623

Harding, G.N., et al., 1958, Second International Conference on the Peaceful Uses of Atomic Energy, Geneva, 1958. Proceedings, 32, 365.

Harvey, A.F., 1963, Microwave engineering, chapter 13. (London, Academic Press).

Hotston, E.S., 1961, J. Sci. Instrum., 38, 130.

Ratcliffe, J.A., 1959, Magneto-ionic theory and its applications to the ionosphere, chapter 6. (Cambridge, University Press).

Redheffer, R.M., 1947, In: Montgomery, C.G., ed. Technique of microwave measurements, chapter 10. (New York, McGraw-Hill).

Von Hippel, A.R., ed., 1954, Dielectric materials and applications. (M.I.T. Technology Press).

Wort, D.J.H., 1963, Refraction of microwaves by a plasma cylinder. CLM - R27. (London, H.M.S.O.)

Wharton, C.B., 1961, In: Drummond, J.E., Plasma Physics, chapter 12, (New York, McGraw-Hill).

TABLE I

MEASURED VALUES OF PHASE SHIFT AND REFRACTIVE INDEX FOR BLOCKS OF POLYSTYRENE FOAM OF THICKNESS ℓ

	$\theta°$ equation 3			$\theta°$ equation 10			$(\mu - 1)10^3$		
Mc/s	ℓcm 5	10	20	5	10	20	5	10	20
8080	3.9	7.6	15.3	4.2	8.3	16.2	8.7	8.6	8.4
9410	5.0	10.4	19.1	5.4	11.0	20.7	9.6	9.7	9.2
11510	5.8	11.8	23.2	6.3	12.8	24.6	9.1	9.3	8.9

Each entry for $\theta°$ is the mean for several determinations all of which lie within $\pm$ 0.4° of the mean

TABLE II

VALUES OF PHASE SHIFT AND DIELECTRIC CONSTANT FOR SINGLE SHEETS OF POLYSTYRENE AND POLYTHENE WHEN INSERTED BETWEEN THE INTERFEROMETER HORNS

f Mc/s	Material	Range of z cm	ℓ cm.	Mean $\theta°$	Mean deviation of $\theta°$	$\mu^2 = Kr$
11560	Polythene	10.2 - 13.7	.3119	25.5	3.1	2.39
8010	Polythene	10 - 13.7	.3119	19.4	1.4	2.43
9370	Polythene	8.8 - 14.7	.3119	21.2	2.4	2.38
9310	Polystyrene	8.5 - 13.5	.5893	40.2	1.6	2.66

ℓ = thickness of plastic sheet

z = separation of plastic sheet from transmitting horn

TABLE III

VALUE OF SIN θ MEASURED FOR RECTANGULAR BLOCKS OF POLYSTYRENE FOAM OF THICKNESS 10 cm AND SIDES a, b WITH SIDE b PARALLEL TO THE ELECTRIC VECTOR, (SIN θ FROM EQUATION 10)

Sin θ								
a (cm) \ b (cm)	5	7	8	9	11	13	15	30
7	.18	.21		.20	.18	.19		
8							.21	
9	.18	.22		.20	.19	.19		
11	.19	.22		.20	.18	.18	.187	
13	.17	.22		.19	.18	.19		
15			.22		.18			
30							.174	.187

f = 9310 Mc/s

TABLE IV

VARIATION OF THE CORRECTION FACTOR C WITH THE OPEN CIRCUIT OUTPUT VOLTAGE OF A CRYSTAL DETECTOR FOR A VALUE OF θ OF 30°

Output voltage	0.03	0.06	0.14	0.25	0.28
C	0.94	0.83	0.74	0.65	0.63

TABLE V

VALUE OF PHASE SHIFT AND PEAK ELECTRON DENSITY FOUND FOR THE M.T.S.E. PLASMA

(The electron density n is calculated for a uniform plasma of 10 cm thickness the errors given for n are the 68% confidence limits assuming a normal distribution for the observations).

No. of shots	θ^{o}				n
	frequency Mc/s	Mean	Mean Deviation	Standard Deviation	peak electron density per c.c. x 10^{-10}.
9	9395	27.6	7.8	10.4	5.3 ± 0.7
13	9412	24.1	7.0	8.6	4.6 ± 0.4

Mean peak value of $n = (4.9 \pm 0.4)\ 10^{10}$/cc

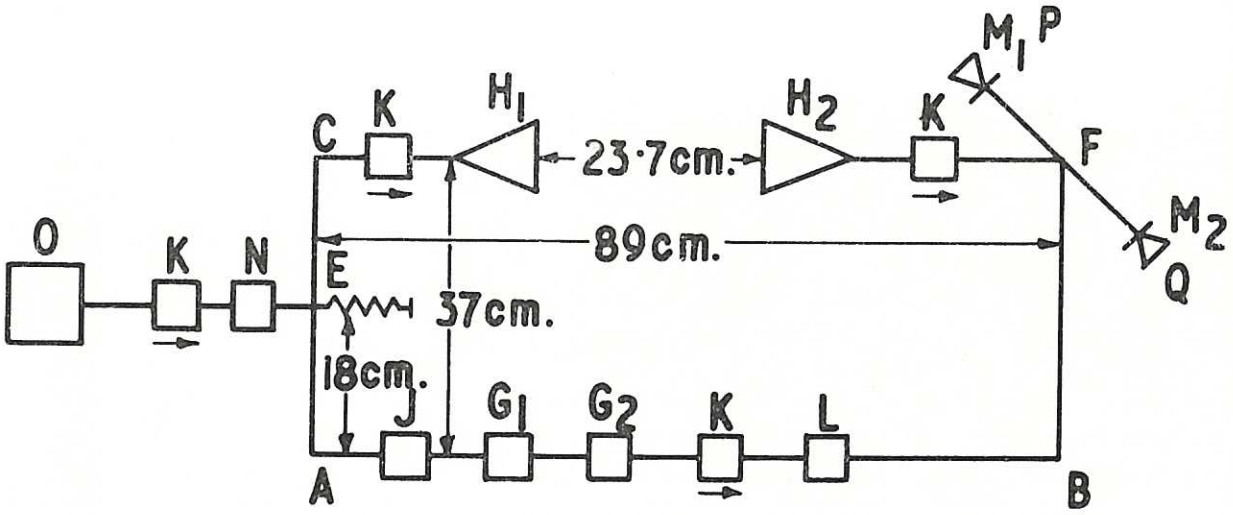

CLM-P62 Fig. 1

Schematic diagram of the interferometer used for the direct current calibration. E, hybrid tee used as beam splitter; F, hybrid tee detector; G_1, G_2, variable attenuators; H_1, H_2, waveguide horns; J, phase shifter; K, ferrite isolators; L, absorption wavemeter; M_1, M_2, crystal detectors; N, level setting attenuator; 0, klystron oscillator

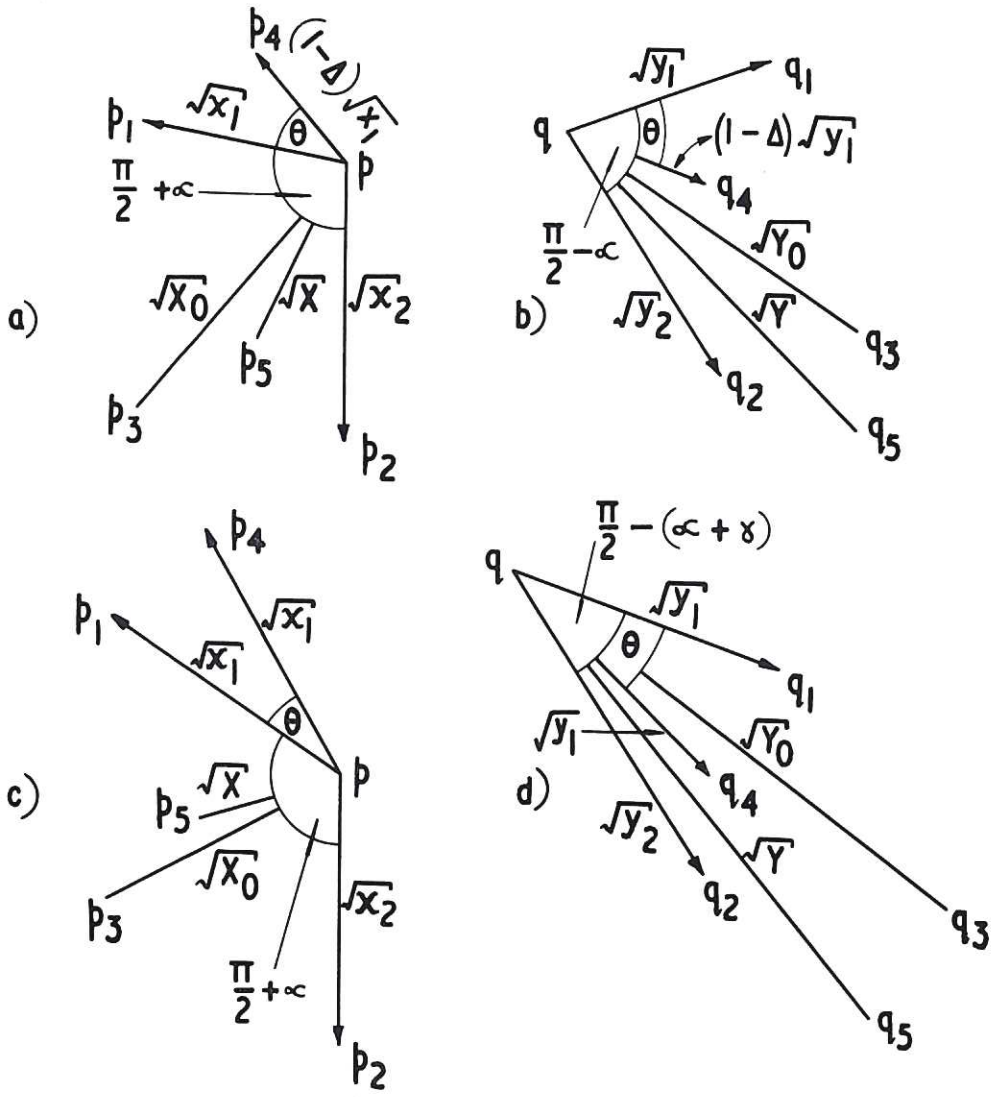

CLM-P62 Fig. 2

Index diagram for the component waves in the waveguides FP, FQ; figures a, c refer to FP; b, d to FQ. The line pp_3 is the resultant of pp_1 and pp_2; and pp_5 that of pp_2 and pp_4; a similar relation holds for the lines qq_1, --, qq_5

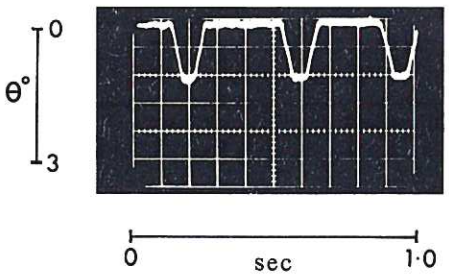

CLM-P62 Fig. 3

Oscillogram showing the phase shift produced by passing a polystyrene foam sheet 1.2 cm thick through the probe beam. (Duration of time base 1 sec)

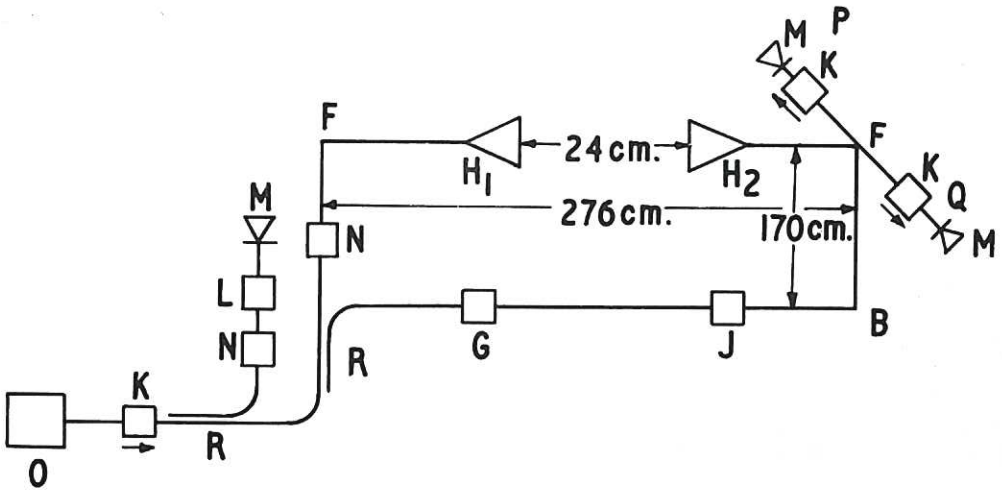

CLM-P62 Fig. 4

Schematic diagram of the interferometer used with the MTSE apparatus. F, hybrid tee detector; G, variable attenuator; H_1 H_2, waveguide horns; J, phase shifter; L, absorption wavemeter; M, crystal detector; N, variable attenuator, P, oscillator; R, directional coupler

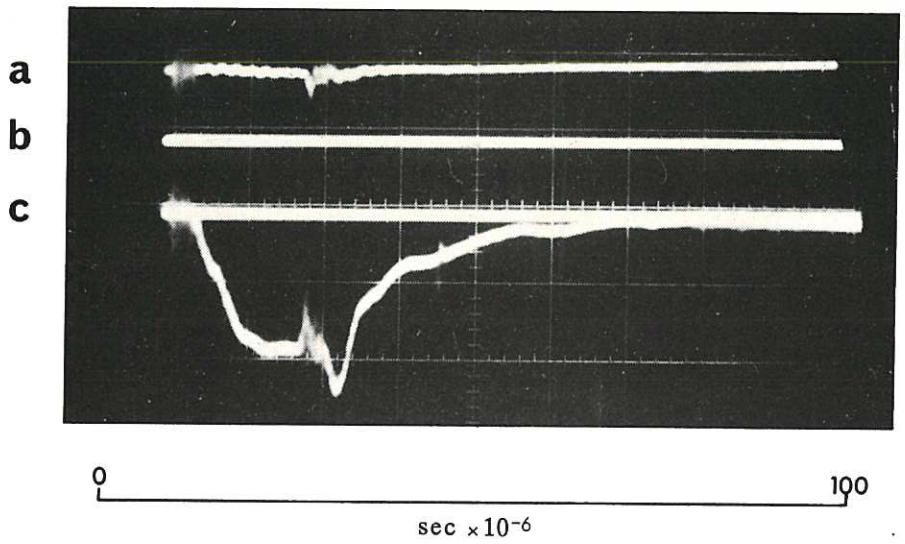

CLM-P62 Fig. 5

Typical oscillogram obtained with the MTSE apparatus; a is the sum signal; b the base line of the sum signals; c the difference signal and its base line. The base lines were obtained with the klystron switched off.